


Stereotactic Body Radiotherapy and Conventional Radiotherapy Induce Cytoskeleton Extension and Enlargement of Cell Morphology in Non-Small Cell Lung Cancer

Dose-Response:
An International Journal
October-December 2021:1–8
© The Author(s) 2021
Article reuse guidelines:
sagepub.com/journals-permissions
DOI: 10.1177/15593258211064499
journals.sagepub.com/home/dos


Xiao Wang^{1,#}, Yanwei Lu^{2,#}, Zhiquan Qin¹, Haiwei Guo³, Wenjuan Chen⁴, Ting Ding⁵, Jianming Tang⁶ and Haibo Zhang²

Abstract

Stereotactic body radiotherapy (SBRT) is now widely used in cancer therapy. However, the biological effects of SBRT compared with conventional radiotherapy (CRT) are not clear. The cytoskeleton plays an important role in many biological processes and cellular life activities. The effects of SBRT or CRT on the morphology and cytoskeletal structure of non-small cell lung cancer (NSCLC) cells remain unknown. Based on the biologically equivalent dose (BED) formula, we designed SBRT and CRT fractionation regimens with the same BED. The morphology was captured during radiation, and rhodamine-phalloidin immunofluorescence was used to study the cytoskeleton. A lactate dehydrogenase assay kit was used to determine the cell membrane permeability, and western blot was used to detect the cytoskeleton protein expression levels. The morphology and cytoskeleton expanded after SBRT or CRT, with an increase in cell membrane permeability and stable cytoskeleton protein levels. Besides, different dose of SBRT (10,20,30 Gy) induce similar morphology and cytoskeleton enlargement. Our findings indicate that SBRT and CRT can induce cytoskeleton reorganization and the enlargement of cell morphology (at different rates) in NSCLC. The morphology and cytoskeleton enlargement after SBRT are dose independence.

Keywords

stereotactic body radiotherapy, conventional radiotherapy, morphology, cytoskeleton, non-small cell lung cancer

Introduction

Radiation plays an important role in cancer treatment, and almost half of cancer patients receive radiotherapy.¹ According to the classical “4 Rs” theory and previous clinical experience,

conventional radiotherapy (CRT) typically applies a dose of 1.8–2 Gy per fraction.^{2,3} Owing to the development of radiation therapy equipment, imageology, and the radiation treatment planning system, it is possible to deliver a higher dose (8–30 Gy) in a shorter time; this is known as stereotactic body

¹Oncology Center, Department of Medical Oncology, Zhejiang Provincial People's Hospital, People's Hospital of Hangzhou Medical College, Hangzhou, China

²Oncology Center, Department of Radiation Oncology, Zhejiang Provincial People's Hospital, People's Hospital of Hangzhou Medical College, Hangzhou, China

³Department of Head and Neck Surgery, Zhejiang Provincial People's Hospital, People's Hospital of Hangzhou Medical College, Hangzhou, China

⁴Department of Psychiatry, Sir Run Run Shaw Hospital, Zhejiang University School of Medicine, Hangzhou, China

⁵Department of Endocrinology, Yiyang Central Hospital, Yiyang, China

⁶Key Laboratory of Biotherapy and Regenerative Medicine of Gansu Province, The First Hospital of Lanzhou University, The First Clinical Medical College of Lanzhou University, Lanzhou, China

[#]These authors Contributed Equally to this work

Corresponding Authors:

Haibo Zhang, Department of Radiation Oncology, Zhejiang Provincial People's Hospital, People's Hospital of Hangzhou Medical College, Hangzhou, Zhejiang, China.

Email: zhbdoctor@163.com

Jianming Tang, Key Laboratory of Biotherapy and Regenerative Medicine of Gansu Province, The First Hospital of Lanzhou University, The First Clinical Medical College of Lanzhou University, Lanzhou, China.

Email: 15900792812@163.com



Creative Commons Non Commercial CC BY-NC: This article is distributed under the terms of the Creative Commons Attribution-NonCommercial 4.0 License (<https://creativecommons.org/licenses/by-nc/4.0/>) which permits non-commercial use, reproduction and distribution of the work without further permission provided the original work is attributed as specified on the SAGE and

Open Access pages (<https://us.sagepub.com/en-us/nam/open-access-at-sage>).

radiotherapy (SBRT) or hypofractionated radiation therapy. SBRT is an accurate and precise technique with high doses for cancer treatment. Recently, SBRT has been widely used for lung cancer, prostate cancer, liver cancer, etc.⁴⁻⁶ However, despite the success of SBRT in the clinical setting, the biological effects of SBRT vs CRT are not fully understood.

According to the classical “4 Rs” theory, the major difference between SBRT and CRT is the delivery of higher doses in less fractions, which results in a high biologically equivalent dose (BED), in SBRT. However, the radiobiological difference between SBRT and CRT when using the same BED is less understood. Our previous study revealed that biological effects such as colony formation, apoptosis, necrosis, senescence, DNA damage, proliferation, and invasion capability differ after SBRT and CRT.⁷ This study focused on changes in cell morphology and cytoskeleton rearrangement after SBRT and CRT. To reduce the interference of intrinsic radiosensitivity on the results, we selected two non-small cell lung cancer (NSCLC) cell lines, A549 and H460, with different radiosensitivities. According to the literature, the α/β value of A549 is 12.40 and that of H460 is 2.95.^{8,9}

The cytoskeleton is a dynamic three-dimensional structure that plays an important role in many biological processes and cellular life activities. Cytoskeletons are composed of three cytoskeletal polymers—actin filaments, intermediate filaments, and microtubules—acted on by three families of motor proteins (dynein, kinesin, and myosin, respectively).¹⁰ We selected β -actin, β -tubulin, and KRT8 as the respective proteins of actin filaments, microtubules, and intermediate filaments.¹¹ Cytoskeleton rearrangement is the structural basis for the exchange of intracellular and extracellular information after radiation.¹² The cytoskeleton is mainly composed of actin microfilaments, and provides a mechanical support framework for maintaining cell morphology, and endothelial integrity and repair.¹³ The cytoskeleton also plays a vital role in cell adhesion, proliferation, motility, differentiation, division, etc.^{14,15} Owing to its importance for cell survival, some microtubule-targeting drugs are widely used to control cancer cell proliferation.¹⁵

External stimuli, such as radiation, photobiomodulation, and acoustic mechanical stress, can induce cytoskeleton reorganization.¹⁶⁻¹⁸ Through cytoskeleton reorganization and dynamic changes, cancer cells can recognize these stimuli and alter gene expression and cell signaling.¹⁹ These stimuli promote cytoskeleton reorganization, thereby altering cancer cell biological processes and cell functions.¹⁹ Although radiotherapy is currently one of the most effective treatments for cancer, the effects of X-ray irradiation (SBRT and CRT) on the cytoskeleton and morphology architecture are poorly understood.

In this study, we investigated the effects of X-ray irradiation on the morphology and cytoskeletal structure of NSCLC cells in SBRT and CRT models with the same BED. Additionally, we examined whether the changes in membrane permeability and cytoskeleton protein levels after SBRT and CRT were the possible mechanisms for these effects. This research provided a new insight into the biological difference between SBRT and CRT; this might help refine radiotherapy treatment in the future.

Materials and Methods

Cell Lines and Culture

The human NSCLC cell lines, A549 and H460, were obtained from ATCC (Gaithersburg, MD, USA). The NSCLC cells were cultured in RPMI 1640 medium (Hyclone™ Laboratories, Logan, UT) supplemented with 10% fetal bovine serum and 1% penicillin/streptomycin (Hyclone™ Laboratories), using a professional cell incubator at 37°C and 5% CO₂ under a fully humidified atmosphere.

See [Supplementary File 1-4](#) for more detailing.

Radiation

Cells were divided into three groups: control group, CRT group, and SBRT group. As cell lines from different laboratories may exhibit subtle differences in radiosensitivity, we used colony-forming and linear-quadratic assays. We established a model to determine the α/β values of the A549 and H460 cell lines in our lab. Through colony formation experiments, we determined that the α/β values of A549 and H460 cells were 10.11 and 3.07, respectively, in our previous study.⁷ Based on the BED formula, $BED = nd(1 + d/(\alpha/\beta))$, and the different α/β values, we designed two fractionation regimens with the same BED: A549-SBRT, 10 Gy/1fx/1w; A549-CRT, 16 Gy/8fx/2w; H460-SBRT, 10 Gy/1fx/1w; and H460-CRT, 26 Gy/13fx/3w. A 6 MV X-ray linear accelerator with a 200 Mu/min dose rate (Primus, Siemens AG, Erlangen, Germany) was used for both SBRT and CRT. To maintain consistency with clinical radiotherapy, the CRT group received radiation from Monday to Friday, and not on weekends. In order to study the biological effects of different SBRT dose, 10 Gy, 20 Gy, 30 Gy were selected. The daily radiotherapy schedule is shown in [Supplementary File 1](#).

Morphology

NSCLC cells were cultured in 6-well plates (Corning Inc., Corning, NY). The cell number per well was 50 000 in the beginning. When the cancer cells were in the logarithmic phase, they were subjected to radiation according to different radiation regimens with the same BED value. All cells kept in the same culture dish without any separation during the 15 consecutive culture days. Cell morphology was captured at a magnification of $\times 100$ using an inverted phase contrast microscope (Olympus America Inc., Melville, NY) for 15 consecutive days. The cell area was analyzed using ImageJ software (version 1.8.0; National Institutes of Health) with 50 cells per group chosen randomly.

Cytoskeleton

Rhodamine-phalloidin immunofluorescence was used to study the cytoskeleton. NSCLC cells after SBRT and CRT were seeded onto sterile cover slips, incubated overnight, and fixed in 4% formaldehyde. After washing with phosphate-buffered saline (PBS) thrice, the cells were permeabilized using .1% Triton X-100. After washing thrice with PBS again, 100 nM rhodamine-phalloidin

(Abcam, Cambridge, England) was used to dye the cells for 30 min at room temperature (RT). After washing thrice with PBS, the cells were treated with DAPI for 10 min, and the slides were mounted using 5% glycerol. Detection time was 24h after the final fraction for A549 and H460 cells. Images were captured at a magnification of $\times 200$ with a Zeiss scanning confocal microscope (Carl Zeiss AG, Oberkochen, Germany) and Olympus FV500 microscope (Olympus America Inc.).

Cell Membrane Permeability

The cell membrane permeability after radiation was tested using a lactate dehydrogenase (LDH) assay kit (Beyotime, Nanjing, China), according to the manufacturer's instructions, with 5 h incubation. LDH release percentage (%) = (OD value of experimental group – OD value of blank)/(OD value of maximum LDH release of experimental group – OD value of blank) $\times 100\%$. Detection time was 24h after the last fraction for A549 and H460 cells. The experiment was repeated thrice.

Western Blot (WB) Analysis

NSCLC cells were lysed in lysis buffer (RIPA buffer and 1% PMSF) (Beyotime) on ice. Then, the cell lysate was sonicated for 15 s and centrifuged at 12 000 r/min for 15 min. The protein concentrations were quantified using the BCA reagent (Ap-plygen Technologies, Beijing, China). The whole-cell extracts were boiled for 5 min in sodium dodecyl sulfate–polyacrylamide gel electrophoresis (SDS-PAGE) buffer (Beyotime). The samples were separated in 8–12% SDS–polyacrylamide gels and electrotransferred to polyvinylidene difluoride membranes. After blocking with 8% non-fat milk in Tris-buffered saline Tween, the membranes were probed overnight with the following antibodies at 4°C: GAPDH (Abcam), β -tubulin (ABclonal, Seoul, Korea), β -actin (Abcam), and KRT8 (ABclonal). The membranes were then incubated with horseradish peroxidase-conjugated goat anti-rabbit and goat anti-mouse (Abcam) secondary antibodies at RT for 1 h. Finally, an enhanced chemiluminescence detection kit (Beyotime) was used to visualize the immunoreactive proteins.⁷

Statistical Analysis

Data from at least three independent experiments with duplicate determinations were expressed as means \pm SEM. Student's t-test or the analysis of variance test was used to determine the statistical significance with GraphPad Prism 6 software (LaJolla, CA). $P < .05$ was considered to indicate a statistically significant difference.

Results

Enlargement of Cell Morphology During SBRT and CRT

During SBRT and CRT, the obvious changes in cell morphology attracted our attention. Hence, we took photos for 15

consecutive days and found that the sizes of A549 and H460 cells increased gradually during radiation. The morphology expanded in both the A549 and H460 cell lines after the radiation regimens of SBRT and CRT (Figures 1A and 1B). For A549 cells, the final area of the cell was $8240.83 \pm 383.61 \mu\text{m}^2$ after SBRT and $8202.16 \pm 421.66 \mu\text{m}^2$ after CRT; the control group area was $1264.40 \pm 58.28 \mu\text{m}^2$. The increase was 6.52-fold for SBRT/control and 6.49-fold for CRT/control in the A549 cell line (Figure 1C). For H460 cells, the final area of the cell was $8022.02 \pm 411.51 \mu\text{m}^2$ after SBRT and $8081.11 \pm 407.31 \mu\text{m}^2$ after CRT; the control group area was $1303.52 \pm 73.53 \mu\text{m}^2$. The increase was 6.15-fold for SBRT/control and 6.14-fold for CRT/control in the H460 cell line (Figure 1D). The sizes of NSCLC cells from the SBRT group increased faster than those from the CRT group during radiation. Finally, the sizes of NSCLC cells from the two groups became similar, and almost 6 times their original values.

Extension of Cytoskeleton After SBRT and CRT

The cytoskeleton helps establish the shapes of cells.¹⁰ Rhodamine-phalloidin is generally used to study the cytoskeleton.²⁰ Hence, we used rhodamine-phalloidin immunofluorescence to detect changes in the cytoskeleton. After SBRT and CRT, we found expansions of cell skeletons in both A549 and H460 cells (Figure 2). The results suggested that the enlargement of cell morphology was due to the extension of the cytoskeleton.

Increase in Cell Membrane Permeability After SBRT and CRT

LDH is a soluble enzyme that is located in the cytosol; it can be released into the surrounding culture medium when cells suffer damage or undergo lysis. Therefore, the LDH activity in the culture medium can be used to measure the plasma membrane permeability, and as an indicator of cell membrane integrity.²¹ The LDH release percentage increased obviously for both A549 and H460 cells after SBRT and CRT. This revealed that radiation increased cell membrane permeability in the A549 and H460 cell lines (Figures 3A and 3B). These data suggest that both SBRT and CRT can destroy cell membrane integrity and increase permeability.

Detection of Cytoskeleton Protein Levels After SBRT and CRT

We investigated the mechanism of cytoskeleton swelling, that is, whether cytoskeleton protein levels increase or the skeleton simply stretches. WB showed that the amount of cell skeleton protein did not increase despite enlargement of the skeleton (Figure 4). This result suggested that the increase in cell size was due to the swelling of the cytoskeleton and increase in

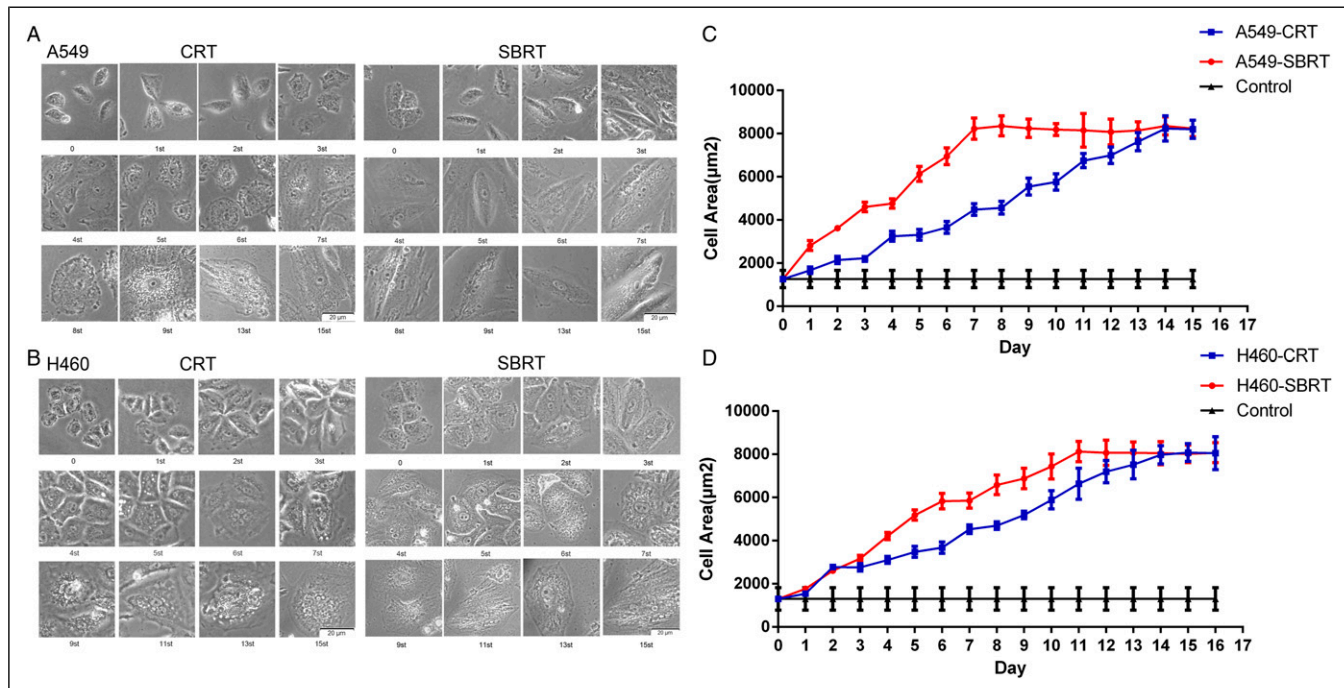


Figure 1. Enlargement of cell morphology during SBRT and CRT. A-B, Images captured during SBRT (10 Gy) and CRT of A549 and H460 cell lines. The images of cell morphology were taken consecutively for 15 days using an Olympus microscope at a magnification of $\times 100$. All cells kept in the same culture dish without any separation during the 15 consecutive culture days. C-D, Area of cells in A549 and H460 cell lines calculated using ImageJ with 50 cells chosen randomly. SBRT enlarged cell morphology faster than CRT. SBRT= Stereotactic body radiotherapy; CRT= conventional irradiation.

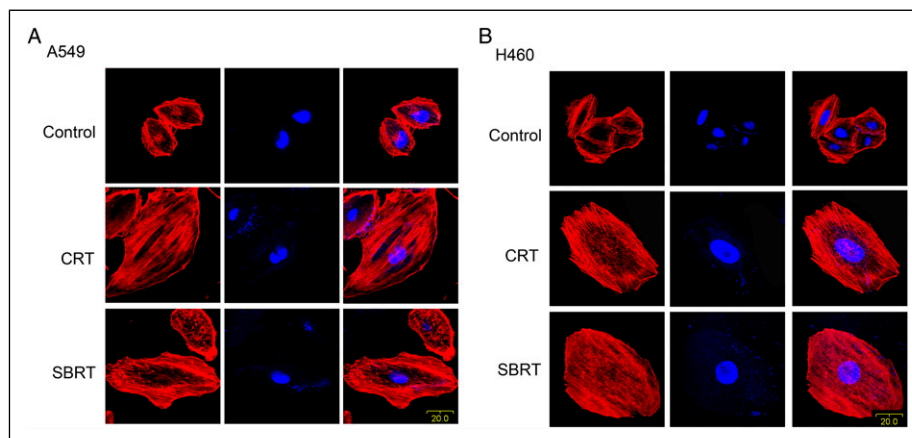


Figure 2. Extension of cytoskeleton after SBRT and CRT. A-B, Cytoskeletons were visualized using rhodamine-phalloidin immunofluorescence; the nuclei are depicted in blue and cytoskeletons in red. The cytoskeletons of A549 and H460 cells expanded after both SBRT (10 Gy) and CRT. The images were captured at a magnification of $\times 200$. SBRT and CRT both extend the cytoskeleton similarly.

permeability of the cellular membrane without cell skeleton protein amplification.

Different Dose of SBRT Induce Enlargement of Cell Morphology and Extension of Cytoskeleton

We investigated whether enlargement of cell morphology and extension of cytoskeleton will be different in different dose.

The SBRT doses were 10 Gy, 20 Gy, 30 Gy. The data showed that the enlargements of cell morphology are similar at 10 Gy, 20 Gy, 30 Gy dose groups and all reached almost 6 times their original size values. For A549 cells, the final area of the cell was $8188.39 \pm 272.61 \mu\text{m}^2$ after SBRT-10 Gy, $8228.97 \pm 334.54 \mu\text{m}^2$ after 20 Gy, and $8565.12 \pm 206.13 \mu\text{m}^2$ after 30 Gy, while the control group is $1264 \pm 58.28 \mu\text{m}^2$ (Figure 5A). For H460 cells, the final area of the cell was $8070.86 \pm$

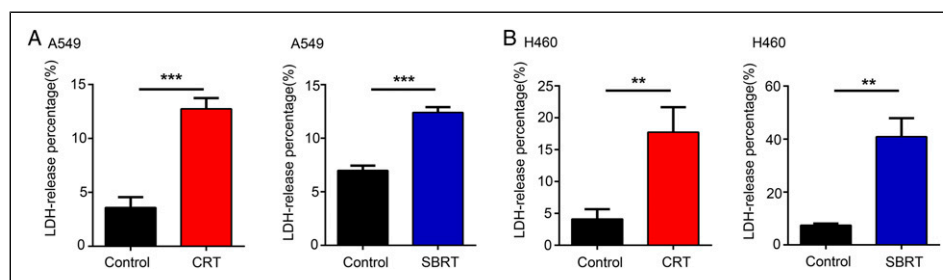


Figure 3. Increase in cell membrane permeability after SBRT and CRT. A-B, The cell membrane permeability was determined using an LDH assay kit; The LDH release ratio was calculated when tumor cells reached their largest sizes after radiation. * $P < .05$, ** $P < .01$, *** $P < .001$. Data represent three independent experiments. SBRT (10 Gy) and CRT increased cell membrane permeability in the A549 and H460 cell lines.

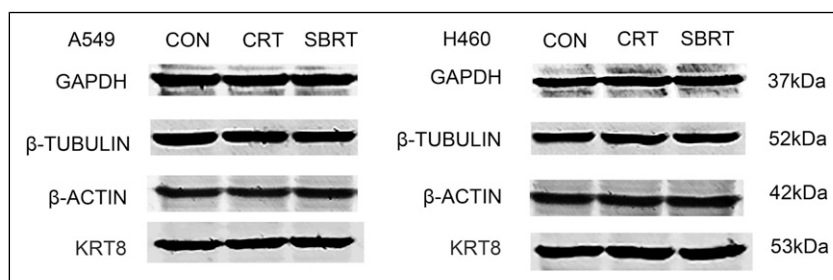


Figure 4. Detection of cytoskeleton protein level after SBRT and CRT. The protein was extracted 24h after SBRT (10 Gy) and CRT. Western blot was used to detect the expression of the cytoskeleton-related proteins, β -tubulin, β -actin, and KRT8, with GAPDH as an internal normalization control in A549 and H460 cells. Western blot revealed that cell skeleton protein β -actin, β -tubulin, and KRT8 did not increase.

504.17 μm^2 after SBRT-10 Gy, 7955.48 \pm 441.54 μm^2 after 20 Gy and 8009.59 \pm 283.03 μm^2 after 30 Gy, while the control group is 1303.52 \pm 73.53 μm^2 (Figure 5B). Besides, the cytoskeletons of A549 and H460 cells also expanded after SBRT (10 Gy, 20 Gy, 30 Gy dose) (Figure 5C-D). The results suggested that the enlargement of cell morphology and cytoskeleton are dose independent.

Discussion

Advances in radiotherapy equipment and technology have made it possible to deliver radiation with a higher dose for a lesser fraction in shorter time than with CRT. SBRT can deliver one or a few large dose fractions of 8–30 Gy per fraction with an acceptable level of normal tissue injury, through high accuracy, reduced margins, and high dose conformation.²² SBRT is rapidly becoming a widely accepted practice for radiation therapy of tumors, especially NSCLC.²³ SBRT has become a standard treatment for early-stage non-operable patients.²⁴ However, the radiobiological principles of SBRT have not been clearly defined, and further research is required to determine its biological advantage over CRT. Through a better understanding of how high doses of ionizing radiation act and the differences between SBRT and CRT, doctors will know exactly what needs to be done to improve the radiotherapy effect, making it possible to refine

radiotherapy treatments in the future.^{22,25} This study explored the differences in cell morphology and cytoskeleton between SBRT and CRT radiobiology; the results may help us understand more about the radiobiological characteristics of different radiotherapy fractionation schedules.

Cells need protein polymers to form a cytoskeleton, which helps establish the cell morphology.¹⁰ The cytoskeleton is a distinctive and dynamic network of interconnected polymers, which contain actin filaments, intermediate filaments, and microtubules.²⁶ The cytoskeleton maintains cell morphology, intracellular transportation, cell division, and other cell life processes.^{10,26} In addition, the cytoskeleton also participates in phagocytosis, cell proliferation, cell migration and invasion, secretion, pinocytosis, and intracellular signal transduction.^{19,27,28} Therefore, changes in cell morphology and the cytoskeleton would affect cellular function and cellular life activity.

Microfilaments are important components of the cytoskeleton and are composed of actin filaments (F-actin) or globules (G-actin).²⁹ Stimuli can induce the intracellular aggregation of free G-actin, which results in the formation of F-actin.³⁰ Microfilaments play an important role in intercellular connections, maintaining cell morphology, and extracellular matrix adhesion. In addition, microfilaments are sensitive to X-ray irradiation, which modifies the structure and activity of the cell cytoskeleton.¹⁷ Ionizing radiation, for

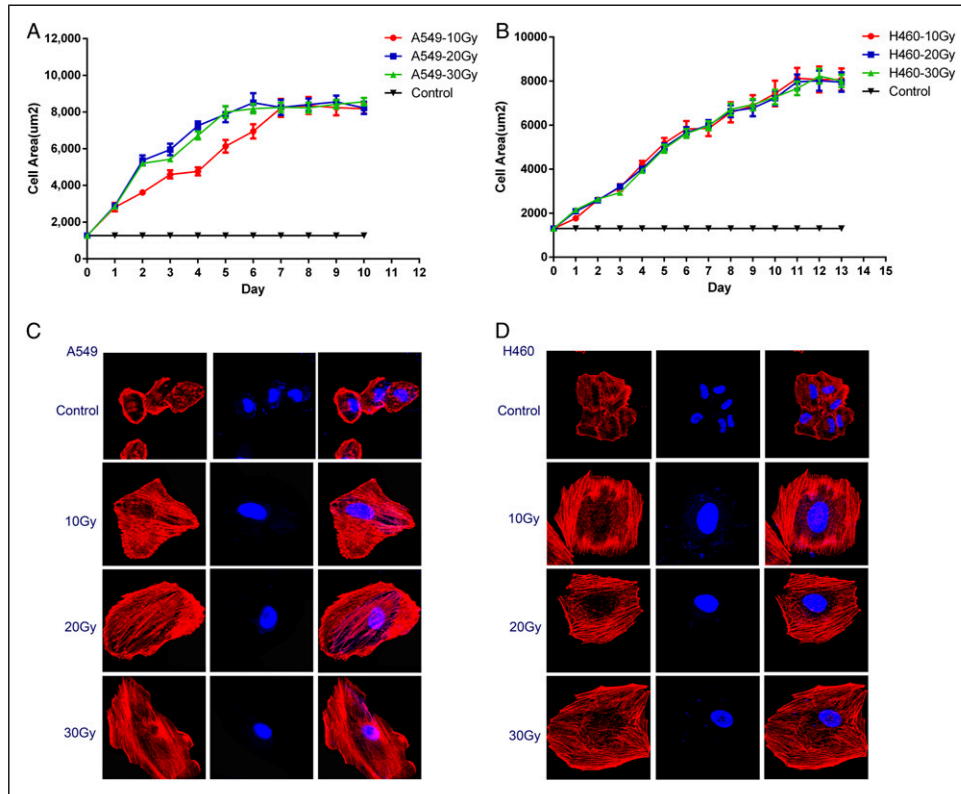


Figure 5. Different dose of SBRT induce enlargement of cell morphology and extension of cytoskeleton. A-B, Images captured after SBRT of 10 Gy, 20 Gy and 30 Gy in A549 and H460 cell lines. C-D, The cytoskeletons of A549 and H460 cells expanded after both SBRT at different dose. The detection time was 10 days after SBRT in A549 cell line and 13 days after SBRT in H460 cell line. The images were captured at a magnification of $\times 200$.

example, a ^{60}Co gamma beam, can alter the cell and nucleus morphology and cytoskeleton organization.³¹ We used rhodamine-phalloidin to dye the F-actin of NSCLC cells, and the results revealed that the cytoskeletons were similarly modified by SBRT and CRT.

Few studies have focused on the effects of SBRT on cell morphology and cytoskeletal structure. In the present study, we firstly investigated changes in the cytoskeleton and morphology of NSCLC cells after SBRT and CRT with the same BED. Owing to the BED effect on X-ray irradiation radiobiology, we designed the radiation regimens for the A549 and H460 cell lines according to the BED formula, to better compare the difference between SBRT and CRT.²⁵ Our study demonstrated that SBRT and CRT both induce cytoskeleton reorganization and morphology changes at different rates. The BED formula quantitatively evaluates the total dose, changes in dose-per-fraction, overall time, and dose rate, and can quantitatively indicate the biological effect of any radiotherapy treatment, such as SBRT and CRT.²⁵ The BED formula based on linear quadratic cell survival in radiobiology is also applicable to biological changes of the cytoskeleton and morphological changes of cells. A difference might occur in the rate of cell morphology enlargement. Our results revealed that SBRT could enlarge the morphology and cytoskeleton

faster than CRT. This indicates that the appropriate time might be different when using drugs, such as some microtubule-targeting drugs, during or after different fractionation regimens.¹⁵

In addition to the enlargement of cell morphology due to cytoskeleton extension, the cytosolic volume greatly increases in a short time. Cells cannot produce sufficient amounts of cytosol to fill the blanks, and extracellular fluid might enter into the cytosol through the cell membrane. This suggests that cell membrane permeability might increase. X-ray or carbon ion irradiation can damage membrane permeability and integrity.³² The LDH release percentage indicated that SBRT and CRT could similarly destroy the cell membrane integrity and increase permeability. In addition to the membrane permeability, cytoskeleton protein levels may be factors associated with cytoskeleton swelling. However, WB results revealed that the levels of the skeleton proteins β -tubulin, β -actin, and KRT8 did not increase, implying that only skeleton stretching occurred. These results reveal that the membrane permeability increased after SBRT and CRT, and cytoskeleton extension occurred without an increase in cytoskeleton protein levels. Besides, it is interesting to find that the enlargement of cell morphology and cytoskeleton after SBRT at 10-30 Gy were similar. The cell size after radiation

reached almost 6 times their original size values, which seems the maximum of cytoskeleton extension, and higher radiation dose would not increase the cell size any more.

Conclusion

In summary, our study demonstrated that both SBRT and CRT could induce cell morphology enlargement and cytoskeleton reorganization, which were caused by an increase in the permeability of the cellular membrane and cytoskeleton stretching without protein amplification in vitro. The enlargement of cell morphology and cytoskeleton are dose independent. These findings may enable a better understanding of the radiobiology of SBRT and CRT, and may provide a theoretical basis for combination therapy with SBRT/CRT and microtubule-targeting drugs for cancer in the future.

Declaration of Conflicting Interests

The author(s) declared no potential conflicts of interest with respect to the research, authorship, and/or publication of this article.

Funding

The author(s) disclosed receipt of the following financial support for the research, authorship, and/or publication of this article: This study was supported in part by grants from the Zhejiang Health Science and Technology Project (Grant number: 2021KY023, to Xiao Wang; 2022KY596, to Haibo Zhang) and National Natural Science Foundation of China (Grant number: 82003215, to Jianming Tang; 82003236, to Haibo Zhang).

Supplementary material

Supplementary Material for this article is available online.

References

1. Wan C, Sun Y, Tian Y, et al. Irradiated tumor cell-derived microparticles mediate tumor eradication via cell killing and immune reprogramming Published 2020 Mar 25. *Science Advances*. 2020;6(13):eaay9789. doi:10.1126/sciadv.aay9789.
2. Pajonk F, Vlashi E, McBride WH. Radiation resistance of cancer stem cells: the 4 R's of radiobiology revisited. *Stem Cell*. 2010; 28(4):639-648. doi:10.1002/stem.318.
3. Castle KD, Kirsch DG. Establishing the impact of vascular damage on tumor response to high-dose radiation therapy. *Cancer Res*. 2019;79(22):5685-5692. doi:10.1158/0008-5472.CAN-19-1323.
4. Duvergé L, Bondiau P-Y, Claude L, et al. Discontinuous stereotactic body radiotherapy schedule increases overall survival in early-stage non-small cell lung cancer. *Lung Cancer*. 2021; 157:100-108. doi:10.1016/j.lungcan.2021.05.016.
5. Ma TM, Lamb JM, Casado M, et al. Magnetic resonance imaging-guided stereotactic body radiotherapy for prostate cancer (mirage): a phase iii randomized trial Published 2021 May 11. *BMC Cancer*. 2021;21(1):538. doi:10.1186/s12885-021-08281-x.
6. Liu HYh., Lee YyD, Sridharan S, et al. Stereotactic body radiotherapy in the management of hepatocellular carcinoma: an Australian multi-institutional patterns of practice review. *Journal of Medical Imaging and Radiation Oncology*. 2021; 65(3):365-373. doi:10.1111/1754-9485.13184.
7. Zhang H, Wan C, Huang J, et al. In vitro radiobiological advantages of hypofractionation compared with conventional fractionation: early-passage NSCLC Cells are less aggressive after hypofractionation. *Radiat Res*. 2018;190(6):584-595. doi:10.1667/RR14951.1.
8. Yu VY, Nguyen D, Pajonk F, et al. Incorporating cancer stem cells in radiation therapy treatment response modeling and the implication in glioblastoma multiforme treatment resistance. *Int J Radiat Oncol Biol Phys*. 2015;91(4):866-875. doi:10.1016/j.ijrobp.2014.12.004.
9. Jiang L, Xiong X-P, Hu C-S, Ou Z-L, Zhu G-P, Ying H-M. In vitro and in vivo studies on radiobiological effects of prolonged fraction delivery time in A549 cells. *J Radiat Res*. 2013;54(2): 230-234. doi:10.1093/jrr/rrs093.
10. Pollard TD, Goldman RD. Overview of the cytoskeleton from an evolutionary perspective Published 2018 Jul 2. *Cold Spring Harbor Perspectives in Biology*. 2018;10(7):a030288. doi:10.1101/cshperspect.a030288.
11. Aleshcheva G, Wehland M, Sahana J, et al. Moderate alterations of the cytoskeleton in human chondrocytes after short-term microgravity produced by parabolic flight maneuvers could be prevented by up-regulation of BMP-2 and SOX-9. *Faseb J*. 2015;29(6):2303-2314. doi:10.1096/fj.14-268151.
12. Huang Q, Zhou Z, Yan F, et al. Low-dose X-ray irradiation induces morphological changes and cytoskeleton reorganization in osteoblasts. *Experimental and Therapeutic Medicine*. 2020; 20(6):1. doi:10.3892/etm.2020.9413.
13. Hohmann T, Dehghani F. The cytoskeleton-a complex interacting meshwork Published 2019 Apr 18. *Cells*. 2019;8(4):362. doi:10.3390/cells8040362.
14. Pegoraro AF, Janmey P, Weitz DA. Mechanical properties of the cytoskeleton and cells Published 2017 Nov 1. *Cold Spring Harbor Perspectives in Biology*. 2017;9(11):a022038. doi:10.1101/cshperspect.a022038.
15. Karahalil B, Yardım-Akaydin S, Nacak Baytas S. An overview of microtubule targeting agents for cancer therapy. *Arh Hig Rada Toksikol*. 2019;70(3):160-172. doi:10.2478/aiht-2019-70-3258.
16. Panzetta V, De Menna M, Musella I, et al. X-rays effects on cytoskeleton mechanics of healthy and tumor cells. *Cytoskeleton*. 2017;74(1):40-52. doi:10.1002/cm.21334.
17. Tani A, Chellini F, Giannelli M, Nosi D, Zecchi-Orlandini S, Sassoli C. Red (635 nm), Near-Infrared (808 nm) and Violet-Blue (405 nm) Photobiomodulation Potentiality on Human Osteoblasts and Mesenchymal Stromal Cells: A Morphological and Molecular In Vitro Study Published 2018 Jul 3. *Int J Mol Sci*. 2018;19(7):1946. doi:10.3390/ijms19071946.

18. Zhang S, Cheng J, Qin Y-X. Mechanobiological modulation of cytoskeleton and calcium influx in osteoblastic cells by short-term focused acoustic radiation force. *PLoS One*. 2012;7(6): e38343. doi:[10.1371/journal.pone.0038343](https://doi.org/10.1371/journal.pone.0038343).
19. Panzetta V, De Menna M, Musella I, et al. X-rays effects on cytoskeleton mechanics of healthy and tumor cells. *Cytoskeleton*. 2017;74(1):40-52. doi:[10.1002/cm.21334](https://doi.org/10.1002/cm.21334).
20. Shi P, Su Y, Li Y, et al. The alternatively spliced porcine FcγRI regulated PRRSV-ADE infection and proinflammatory cytokine production. *Dev Comp Immunol*. 2019;90:186-198. doi:[10.1016/j.dci.2018.09.019](https://doi.org/10.1016/j.dci.2018.09.019).
21. Haslam G, Wyatt D, Kitos PA. Estimating the number of viable animal cells in multi-well cultures based on their lactate dehydrogenase activities. *Cytotechnology*. 2000;32(1):63-75. doi:[10.1023/A:1008121125755](https://doi.org/10.1023/A:1008121125755).
22. Brown JM, Carlson DJ, Brenner DJ. The tumor radiobiology of SRS and SBRT: are more than the 5 Rs involved?. *Int J Radiat Oncol Biol Phys*. 2014;88(2):254-262. doi:[10.1016/j.ijrobp.2013.07.022](https://doi.org/10.1016/j.ijrobp.2013.07.022).
23. Vlaskou Badra E, Baumgartl M, Fabiano S, Jongen A, Guckenberger M. Stereotactic radiotherapy for early stage non-small cell lung cancer: current standards and ongoing research. *Transl Lung Cancer Res*. 2021;10(4):1930-1949. doi:[10.21037/tlcr-20-860](https://doi.org/10.21037/tlcr-20-860).
24. Mancosu P, Nisbet A, Jornet N. Editorial: the role of medical physics in lung SBRT. *Phys Med*. 2018;45:205-206. doi:[10.1016/j.ejmp.2018.01.001](https://doi.org/10.1016/j.ejmp.2018.01.001).
25. Qiu B, Aili A, Xue L, Jiang P, Wang J. Advances in radiobiology of stereotactic ablative radiotherapy Published 2020 Aug 7. *Frontiers in Oncology*. 2020;10:1165. doi:[10.3389/fonc.2020.01165](https://doi.org/10.3389/fonc.2020.01165).
26. Blanquie O, Bradke F. Cytoskeleton dynamics in axon regeneration. *Curr Opin Neurobiol*. 2018;51:60-69. doi:[10.1016/j.conb.2018.02.024](https://doi.org/10.1016/j.conb.2018.02.024).
27. Wang Y, Shan Q, Pan J, Yi S. Actin cytoskeleton affects schwann cell migration and peripheral nerve regeneration Published 2018 Jan 25. *Front Physiol*. 2018;9:23. doi:[10.3389/fphys.2018.00023](https://doi.org/10.3389/fphys.2018.00023).
28. Szymanski D, Staiger CJ. The actin cytoskeleton: functional arrays for cytoplasmic organization and cell shape control. *Plant Physiology*. 2018;176(1):106-118. doi:[10.1104/pp.17.01519](https://doi.org/10.1104/pp.17.01519).
29. Svitkina T. The actin cytoskeleton and actin-based motility Published 2018 Jan 2. *Cold Spring Harbor Perspectives in Biology*. 2018;10(1):a018267. doi:[10.1101/cshperspect.a018267](https://doi.org/10.1101/cshperspect.a018267).
30. Arnsdorf EJ, Tummala P, Kwon RY, Jacobs CR. Mechanically induced osteogenic differentiation - the role of RhoA, ROCKII and cytoskeletal dynamics. *J Cell Sci*. 2009;122(Pt 4):546-553. doi:[10.1242/jcs.036293](https://doi.org/10.1242/jcs.036293).
31. Mohammadkarim A, Tabatabaei M, Parandakh A, Mokhtari-Dizaji M, Tafazzoli-Shadpour M, Khani M-M. Radiation therapy affects the mechanical behavior of human umbilical vein endothelial cells. *Journal of the Mechanical Behavior of Biomedical Materials*. 2018;85:188-193. doi:[10.1016/j.jmbbm.2018.06.009](https://doi.org/10.1016/j.jmbbm.2018.06.009).
32. Cao G, Zhang M, Miao J, et al. Effects of X-ray and carbon ion beam irradiation on membrane permeability and integrity in *Saccharomyces cerevisiae* cells. *J Radiat Res*. 2015;56(2): 294-304. doi:[10.1093/jrr/rru114](https://doi.org/10.1093/jrr/rru114).